

# High temperature neutron diffraction study of the $\text{Al}_2\text{O}_3\text{--Y}_2\text{O}_3$ system

M. Medraj<sup>a,\*</sup>, R. Hammond<sup>b</sup>, M.A. Parvez<sup>a</sup>, R.A.L. Drew<sup>c</sup>, W.T. Thompson<sup>d</sup>

<sup>a</sup> *Concordia University, Montreal, Que., Canada H3G 1M8*

<sup>b</sup> *NPMR, NRC, Chalk River, Canada*

<sup>c</sup> *McGill University, Montreal, Canada*

<sup>d</sup> *Royal Military College, Kingston, Canada*

Received 12 August 2005; received in revised form 24 November 2005; accepted 3 December 2005

Available online 18 January 2006

## Abstract

The phase diagram of the  $\text{Al}_2\text{O}_3\text{--Y}_2\text{O}_3$  system has been investigated with five different compositions by XRD and in situ high temperature neutron diffractometry. High purity YAG, YAP and YAM compounds have been produced successfully through a melt extraction technique. High temperature neutron diffraction has made it possible to follow, in real time, the reactions involved in this system, especially to determine the temperature range of each reaction, which would have been impossible to determine by other means. A good agreement between the experimental results and the phase diagram of the  $\text{Al}_2\text{O}_3\text{--Y}_2\text{O}_3$  system has been observed.

© 2005 Elsevier Ltd. All rights reserved.

**Keywords:** Neutron diffraction; Powder-solid state reaction;  $\text{Al}_2\text{O}_3$ ;  $\text{Y}_2\text{O}_3$

## 1. Introduction

The importance of the  $\text{Al}_2\text{O}_3\text{--Y}_2\text{O}_3$  phase diagram stems from the significance of alumina and yttria for liquid phase sintering of the covalently bonded ceramic AlN.<sup>1</sup> In the  $\text{Al}_2\text{O}_3\text{--Y}_2\text{O}_3$  system, there are three important compounds:  $\text{Y}_3\text{Al}_5\text{O}_{12}$  (YAG),  $\text{YAlO}_3$  (YAP) and  $\text{Y}_4\text{Al}_2\text{O}_9$  (YAM)<sup>2</sup> having cubic garnet, orthorhombic perovskite and monoclinic structure, respectively. These compounds are of considerable interest as solid-state laser materials.<sup>3–5</sup> Recent studies show that YAG and the  $\text{Al}_2\text{O}_3\text{--YAG}$  eutectic are potential candidate materials for reinforcement fibers in ceramic and intermetallic composites used in structural applications.<sup>6,7</sup> In addition, YAG doped with Nd is widely used as a laser material.  $\text{YAlO}_3$  (YAP) is an excellent material for gain media, scintillators and acousto-optics. Single crystal YAP can be grown by the Czochralski technique or by vertical directional solidification.<sup>8</sup> Yamane et al.<sup>9–11</sup> studied the phase transition of  $\text{Y}_4\text{Al}_2\text{O}_9$  (YAM) by high temperature differential scanning calorimetry (DSC), high temperature X-ray powder diffraction (XRD) and high temperature dilatometry. Their XRD experiments showed no

difference between the diffraction patterns of the high temperature and the room temperature phases.<sup>4,5,9</sup> YAG is the only unambiguously stable phase in the system according to Abell et al.<sup>4</sup> Cockayne<sup>5</sup> reviewed the  $\text{Al}_2\text{O}_3\text{--Y}_2\text{O}_3$  system, and reported the melting points and the stability ranges for the end and stoichiometric compounds that occur in this system.

Lo and Tseng<sup>2</sup> studied the phase evolution of YAG, YAP and YAM synthesized by a modified sol–gel method and used XRD to determine the crystalline phases. They could obtain synthesized high-purity YAG and YAM phases, but they concluded that YAP is a result of reaction between YAG and YAM, where residual amounts were left even after heat treatment. Gervais et al.<sup>12</sup> studied the solidification process of liquid YAG and YAP by differential thermal analysis (DTA) and, unlike Maier and Saviniva,<sup>8</sup> observed difficulties in the growth of single crystals of both YAG and YAP.

Synthesizing YAG, YAM and YAP from the oxides is difficult. YAG synthesized by solid-state reaction contained unreacted  $\text{Y}_2\text{O}_3$  and  $\text{Al}_2\text{O}_3$ . Since alumina and yttria are important for liquid phase sintering of AlN, the need to understand the phase relationships in the  $\text{Al}_2\text{O}_3\text{--Y}_2\text{O}_3$  system becomes more important. In this regard, in situ study of the development and stability of the phases in the  $\text{Al}_2\text{O}_3\text{--Y}_2\text{O}_3$  system should be conducted. In this article, the phase development

\* Corresponding author. Tel.: +1 514 848 2424x3146; fax: +1 514 848 3175.  
E-mail address: [mmedraj@encs.concordia.ca](mailto:mmedraj@encs.concordia.ca) (M. Medraj).

Table 1  
Chemical composition and the expected phases of the studied samples

Sample no.	Al <sub>2</sub> O <sub>3</sub> mol% (wt.%)	Composition
1	79% (62.94%)	e <sub>1</sub>
2	62.5% (42.94%)	YAG
3	57.5% (37.92%)	e <sub>2</sub>
4	50% (31.11%)	YAP
5	33.33% (18.42%)	YAM

was investigated using X-ray diffractometry, XRD, which provided the phases existing at room temperature but not the temperature ranges of the reactions. Hence, phase evolution in Al<sub>2</sub>O<sub>3</sub>–Y<sub>2</sub>O<sub>3</sub> system was studied in situ at elevated temperatures using neutron diffractometry which provided, in real time, information on the reactions and their temperature ranges. The formation of YAG, YAP and YAM will be described. Experimental results were also compared with the Al<sub>2</sub>O<sub>3</sub>–Y<sub>2</sub>O<sub>3</sub> phase diagram.

## 2. Experimental procedures

To determine phase evolution in the Al<sub>2</sub>O<sub>3</sub>–Y<sub>2</sub>O<sub>3</sub> system, the neutron diffraction patterns were monitored in situ at elevated temperature using the DUALSPEC high-resolution powder diffractometer, C2, at the NRU reactor of Atomic Energy of Canada Limited (AECL), Chalk River Laboratories. The major advantage of neutron diffraction compared to other diffraction techniques is the extraordinarily penetrating nature of the neutrons, which leads to its use in measurements under special environments.<sup>13</sup> The diffractometer is an 800-channel position sensitive detector that spans 80° in scattering angle, 2θ. The wavelength, λ, of the neutron beam was calibrated by measuring the diffraction pattern of a standard powder of alumina, obtained from the National Institute of Standards and Technology. λ = 1.33(1) Å and 2θ range from 8° to 88° were used in this experiment. The diffractometer was equipped with a tantalum-element vacuum furnace capable of reaching temperatures as high as 2000 °C. The furnace programming and data acquisition system were fully computerized, allowing accurate temperature control and rapid data collection.

Y<sub>2</sub>O<sub>3</sub> powder, grade 5600, supplied by Union Molycorp, U.S.A. with 99.99% purity and Al<sub>2</sub>O<sub>3</sub> powder, grade A16-SG, supplied by Alcoa Industrial Chemical Division, Canada, with 99.8% purity, were mixed in various stoichiometric amounts. Table 1 and Fig. 1 show the composition of these samples. These samples include two compositions corresponding to eutectic points and three stoichiometric compounds. The premixed compositions were ball milled in a plastic container for 1 h using 4 mm diameter Al<sub>2</sub>O<sub>3</sub> media and water with a solid to liquid ratio of 1:5 by volume. The resultant slurry was dried in a microwave oven to completely remove the water. After drying, the mixtures were granulated through a 60 μm mesh sieve to create a fine powder mixture. A portion of each composition was encapsulated in molybdenum foil to prevent the powder from spreading in the sample chamber upon evacuating, and to protect the appa-

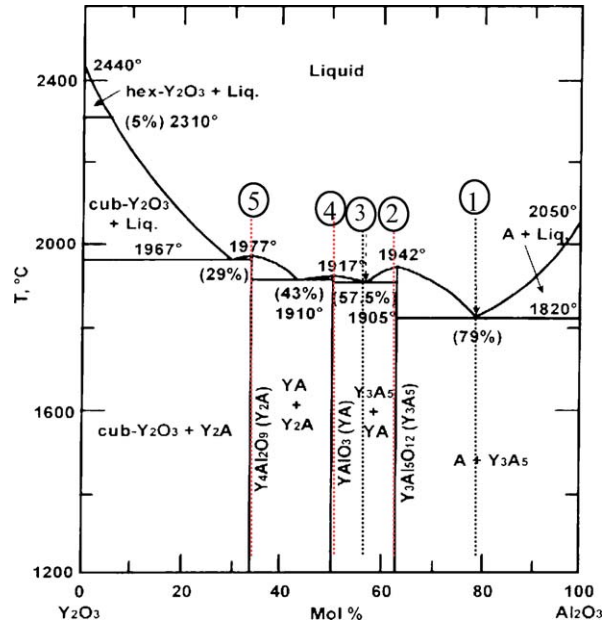


Fig. 1. Experimental Al<sub>2</sub>O<sub>3</sub>–Y<sub>2</sub>O<sub>3</sub> phase diagram<sup>25</sup> with the investigated compositions.

ratus when the sample melts. A neutron diffraction spectrum for each sample was collected at room temperature to form the reference for any reactions taking place upon heating. During heating and cooling, samples were kept under 1 atm of argon gas within the molybdenum tube. The sample was observed in situ during heating and cooling. Neutron diffraction spectra were collected at incremental intervals until the spectra displayed loss of crystallinity or reached the maximum temperature of the apparatus (2000 °C). At each step the temperature was maintained for 120 min to ensure that the reaction was complete. After melting or reaching 2000 °C, cooling started and neutron spectra were collected at incremental cooling temperatures to observe the precipitation of crystalline phases.

The phase development was also investigated at room temperature using X-ray diffraction for different stages of heat treatment. First X-ray diffraction was carried out for the mixed starting powders in their stoichiometric ratio. This was done in order to have a baseline comparison to detect any change and phase development during the later stages of heat treatment. This powder was then mixed with water and 8 wt.% of hydroxypropyl cellulose as a plasticizer and the mixture was extruded into 2.5 mm diameter rods. These rods were dried in air for 24 h. Initially, a solid-state reaction of these powders was performed at 1500 °C for 2 h at a heating rate of 10 °C/min using a silicon carbide element, Blue M furnace. However, it has been found that a solid-state reaction led to an incomplete reaction. This indicated that a different experimental approach was required to bring about complete reaction; therefore, the samples were melted at ~2200 °C using an oxyacetylene torch. The X-ray diffraction was performed on the crushed droplets for each composition. The chemical analysis of Aguilar and Drew<sup>14</sup> showed that there is no contamination or weight loss when this technique was used for the melt extraction of Al<sub>2</sub>O<sub>3</sub>–Y<sub>2</sub>O<sub>3</sub> fibers.

### 3. Results

In this section, five compositions will be discussed followed by a summary and comparison with the  $\text{Al}_2\text{O}_3\text{--Y}_2\text{O}_3$  phase diagram.

#### 3.1. E1 composition

Fig. 2 illustrates the reaction of the E1 composition from room temperature until 1900 °C. The main evolution in the diffraction pattern appears to be the gradual formation of YAG phase, and the gradual reduction in the intensity of the  $\text{Y}_2\text{O}_3$  diffraction peaks with the progression of heating. The reaction of  $\text{Al}_2\text{O}_3$  and  $\text{Y}_2\text{O}_3$  to produce YAG is clearly evident from the new diffraction peaks. These peaks can be seen first at 1200 °C in addition to diffraction peaks for  $\text{Al}_2\text{O}_3$  and  $\text{Y}_2\text{O}_3$  with lower intensities than those at room temperature.  $\text{Y}_2\text{O}_3$  diffraction peaks were not observed at 1500 °C; this means all available  $\text{Y}_2\text{O}_3$  was reacted to produce YAG upon heating from

1200 °C to 1500 °C. Then neutron diffraction data were collected at higher temperature to detect the melting point of this composition. No changes can be seen in the patterns collected in the range of 1500–1850 °C. It can be seen from this figure that the sample lost crystallinity in the diffraction pattern collected at 1900 °C. This means that the sample had melted between 1850 °C and 1900 °C. For all spectra,  $\text{Al}_2\text{O}_3$  peaks and  $\text{Y}_2\text{O}_3$  peaks were identified using a rhombohedral unit-cell (space group  $R\bar{3}c$ ,  $a = 4.759(0)$  Å and  $c = 12.992(0)$  Å)<sup>15–17</sup> and a cubic unit-cell (space group  $Ia\bar{3}$ ,  $a = 10.608(7)$  Å),<sup>17–19</sup> respectively, while YAG peaks were indexed as a cubic unit-cell (space group  $Ia\bar{3}d$ ,  $a = 12.016(3)$  Å).<sup>3,12,20</sup>

Fig. 3 shows the cooling cycle of the E1 composition. It can be seen that YAG and  $\text{Al}_2\text{O}_3$  were fully crystallized at 1600 °C. By cooling from 1600 °C to room temperature, no difference in the collected diffraction patterns was noticed. This indicates that YAG and  $\text{Al}_2\text{O}_3$  are the stable phases for the E1 composition since no further crystallization occurred down to room temperature. Fig. 3 also shows that the peaks shifted to higher diffraction

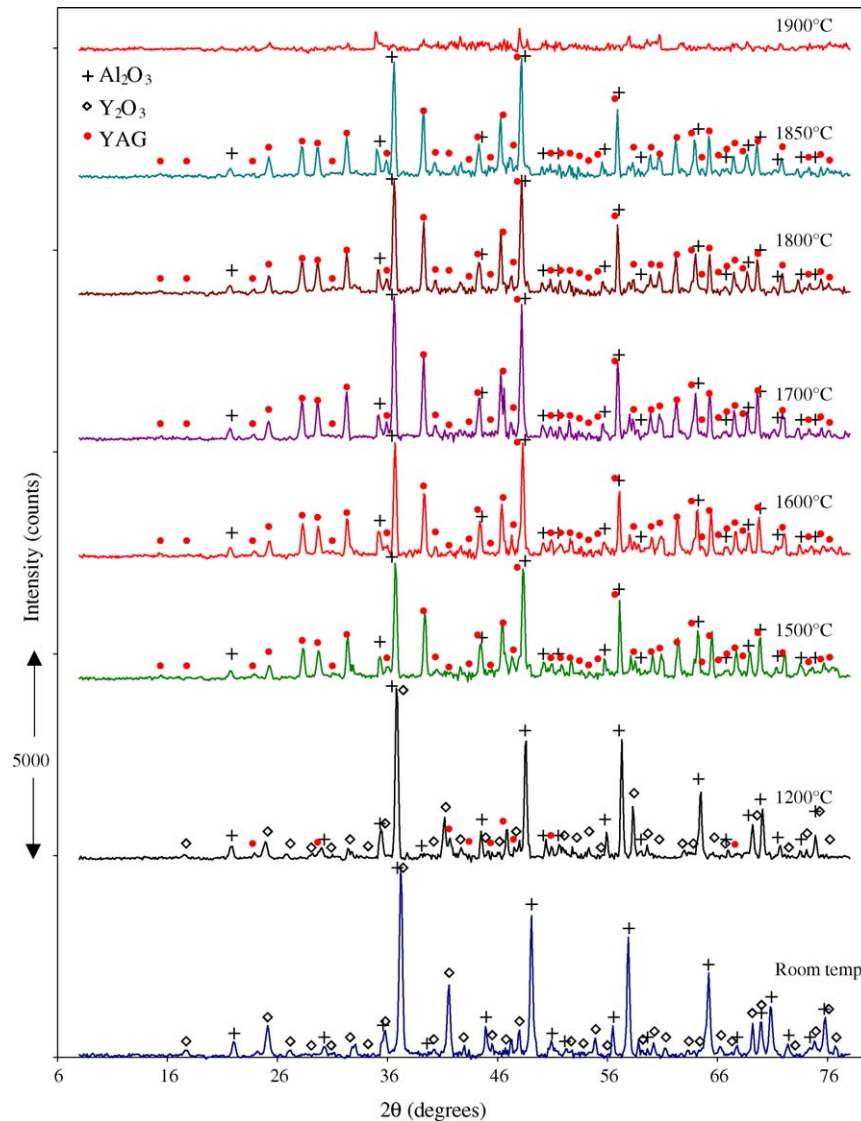


Fig. 2. Neutron diffractograms of heating of E1 composition.

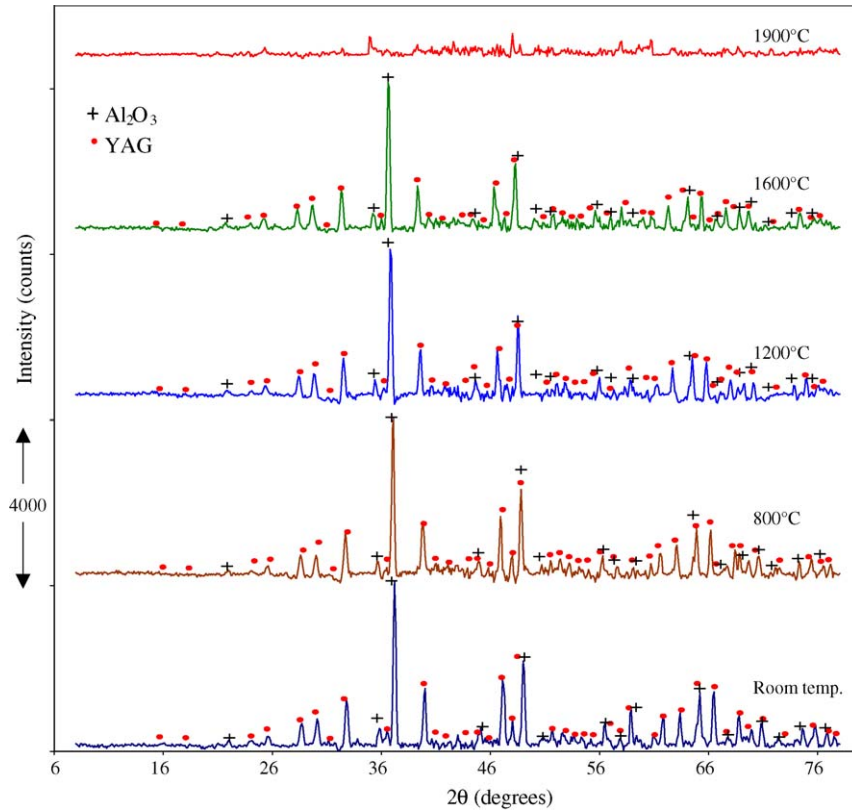


Fig. 3. Neutron diffractograms of cooling of E1 composition.

angle with decreasing temperature. The same phenomenon was also noticed in Fig. 2, where the peaks shifted to lower diffraction angle with increasing temperature. This indicates a positive thermal expansion coefficient for both YAG and Al<sub>2</sub>O<sub>3</sub>.

X-ray diffractograms of the E1 composition are shown in Fig. 4, where Y<sub>2</sub>O<sub>3</sub> peaks were indexed using JCPDS card 25–1200, Al<sub>2</sub>O<sub>3</sub> peaks by JCPDS card 10–173 and YAG peaks were indexed by JCPDS card 33–40. The patterns of the mixed

powder are labeled with the letter (a). Initially, a solid-state reaction of these powders was attempted at 1500 °C for 2 h. X-ray diffraction was conducted at room temperature and the patterns were labeled with the letter (b). The X-ray diffraction was performed on the melted droplets for each composition and the resulting patterns were labeled with the letter (c). All the peaks in pattern (a) in Fig. 5 are related to Y<sub>2</sub>O<sub>3</sub> and Al<sub>2</sub>O<sub>3</sub>. It can be seen that the strong peaks are Y<sub>2</sub>O<sub>3</sub> while the weaker ones cor-

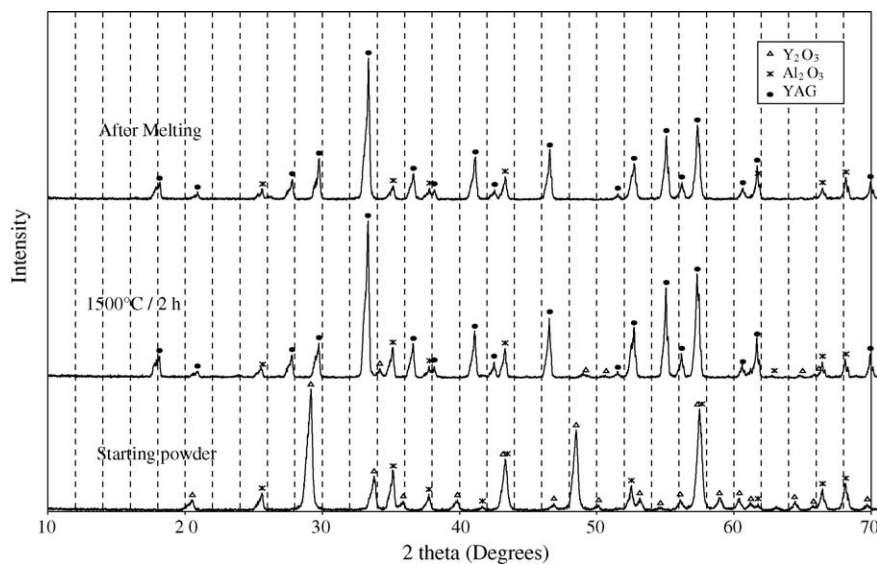


Fig. 4. XRD patterns of E1 composition.

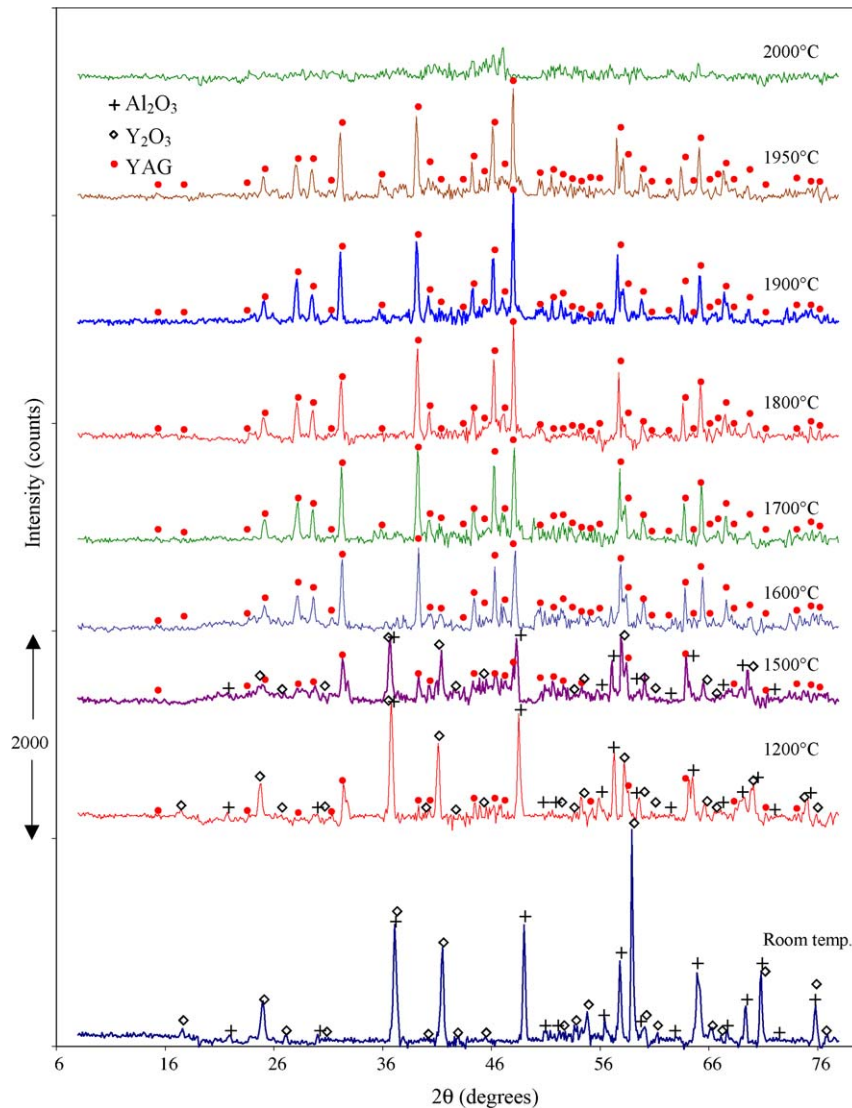


Fig. 5. Neutron diffractograms of heating of YAG composition.

respond to  $\text{Al}_2\text{O}_3$ . This refers to the fact that the atomic number of yttrium is 39 and 13 for aluminum. Pattern (c) in this figure shows that YAG and  $\text{Al}_2\text{O}_3$  are the stable phases after melting and solidification. These results obey the Lever Rule, exhibiting complete consistency with the phase diagram and neutron diffraction results.

### 3.2. YAG composition

Neutron diffraction spectra acquired during heating cycle of sample 2 which has YAG composition are presented in Fig. 5. It can be seen from Fig. 5 that a mixture of 62.5 mol%  $\text{Al}_2\text{O}_3$  and 37.5 mol%  $\text{Y}_2\text{O}_3$  produced a pure YAG phase at 1600 °C. The first changes are already visible when comparing the neutron diffraction patterns of 1200 °C with that at room temperature, where additional peaks, for example at 33° ( $2\theta$ ) and 64° ( $2\theta$ ), appear. These peaks continue to grow, whereas the peaks of  $\text{Al}_2\text{O}_3$  and  $\text{Y}_2\text{O}_3$  decay with increasing temperature up to 1600 °C. For example, the (440) peak of  $\text{Y}_2\text{O}_3$  at 41.5° ( $2\theta$ ),

which does not overlap with other peaks, is still present up to 1500 °C but cannot be observed at 1600 °C and higher. The same phenomenon was observed in the (119) peak of  $\text{Al}_2\text{O}_3$  at 65° ( $2\theta$ ), which indicates that the reaction was completed between 1500 °C and 1600 °C.

The patterns are practically unchanged from 1600 °C up to 1950 °C, if peak shifts due to thermal expansion of the lattice, are neglected. The diffraction pattern collected at 2000 °C in Fig. 5 shows complete loss of crystallinity. This indicates that sample 2 melts between 1950 °C and 2000 °C.

The neutron diffraction patterns of the cooling sequence for sample 2 show a full recrystallization of the YAG phase at 1600 °C. There is no phase transformation or decomposition of YAG upon cooling from its melt.

X-ray diffractograms of YAG composition are shown in Fig. 6. Pattern (b) in Fig. 6 shows that not all the peaks are related to the YAG phase. This indicates that the formation of YAG was incomplete at this temperature. This is consistent with neutron diffraction pattern during heating of this sample. However pat-

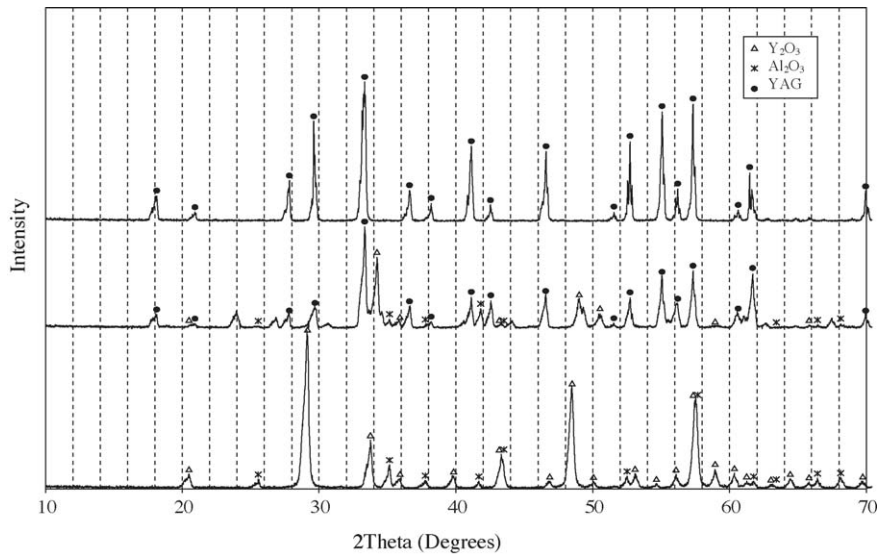


Fig. 6. XRD patterns of YAG composition.

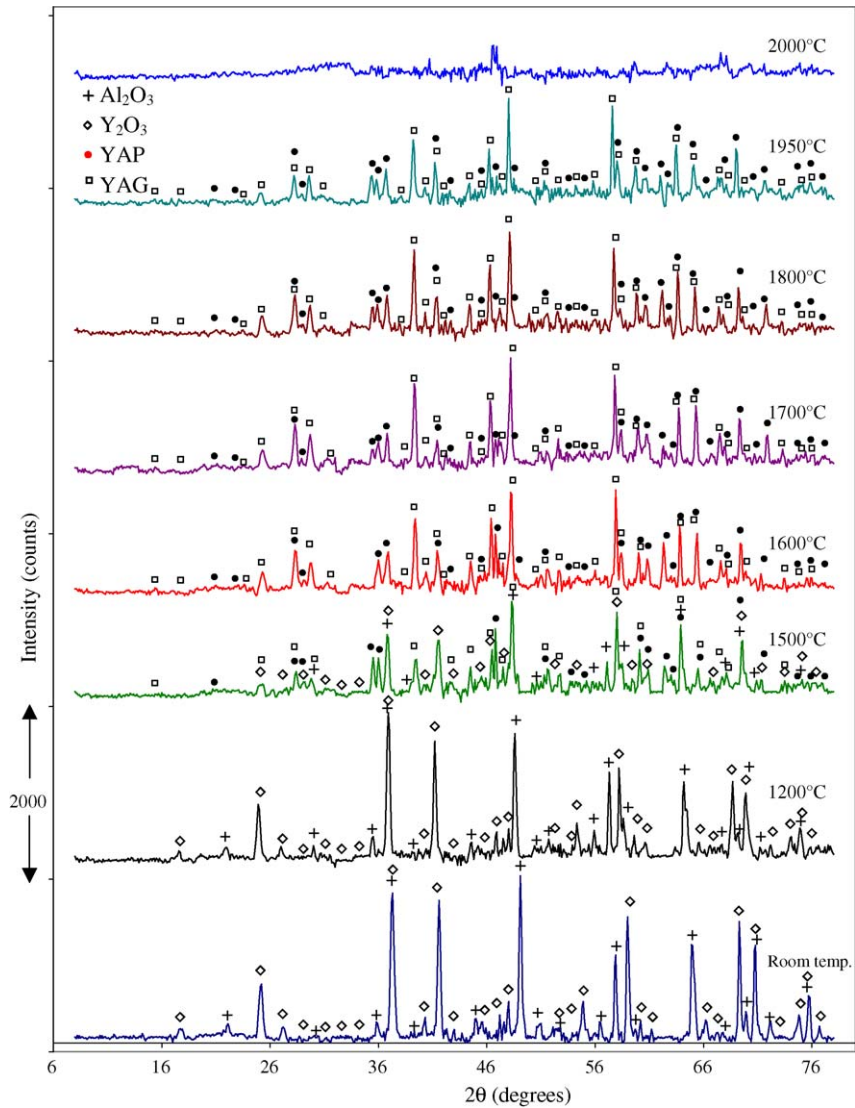


Fig. 7. Neutron diffractograms of heating of E2 composition.

tern (c) shows no residual reactants after melting indicating the formation of pure YAG from this composition.

### 3.3. E2 Composition

The development of the neutron diffraction pattern of E2 composition, representing the second eutectic point in the  $\text{Al}_2\text{O}_3\text{--Y}_2\text{O}_3$  phase diagram, with increasing temperature up to 2000 °C is shown in Fig. 7. Comparing the neutron diffraction patterns at 1200 °C and that at room temperature shows that no additional peaks evolved at 1200 °C. The first changes are visible when comparing patterns at 1500 °C and 1200 °C where additional peaks, for example (4 2 0) of YAG and (2 2 0) of YAP, respectively, at 28° ( $2\theta$ ) and 35° ( $2\theta$ ) appear. This indicates that the reaction started in the temperature range of 1200–1500 °C. At 1500 °C significant proportions of both  $\text{Al}_2\text{O}_3$  and  $\text{Y}_2\text{O}_3$  are present, which are illustrated by, for example, the two overlapping peaks (4 1 3) of  $\text{Y}_2\text{O}_3$  and (1 1 3) of  $\text{Al}_2\text{O}_3$  at 37° ( $2\theta$ ), while there are no  $\text{Al}_2\text{O}_3$  and  $\text{Y}_2\text{O}_3$  traces visible at 1600 °C.

This indicates that the reaction was completed between 1500 °C and 1600 °C. At 1600 °C all the peaks correspond to YAG and YAP phases. YAP peaks were identified as orthorhombic unit-cell (space group  $Pnma$ ,  $a = 5.330(2)$  Å,  $b = 7.375(2)$  Å and  $c = 5.180(2)$  Å).<sup>21–23</sup> The patterns are unchanged up to 1950 °C, if the shifts of reflections due to thermal expansion of the lattice are neglected. It can be seen from this figure that sample 3 was melted in the temperature range of 1950–2000 °C. This sample was also monitored during cooling; YAP and YAG crystallized from the melt and found to be stable down to room temperature.

### 3.4. YAP composition

The reaction process was different when starting with 50 mol%  $\text{Al}_2\text{O}_3$  and 50 mol%  $\text{Y}_2\text{O}_3$ . This was obvious when the collected spectra of this sample at different temperature shown in Fig. 8 were compared. The first changes are already visible by comparing the neutron diffraction patterns of 1500 °C and 1200 °C. The pattern at 1500 °C clearly shows the decay of the

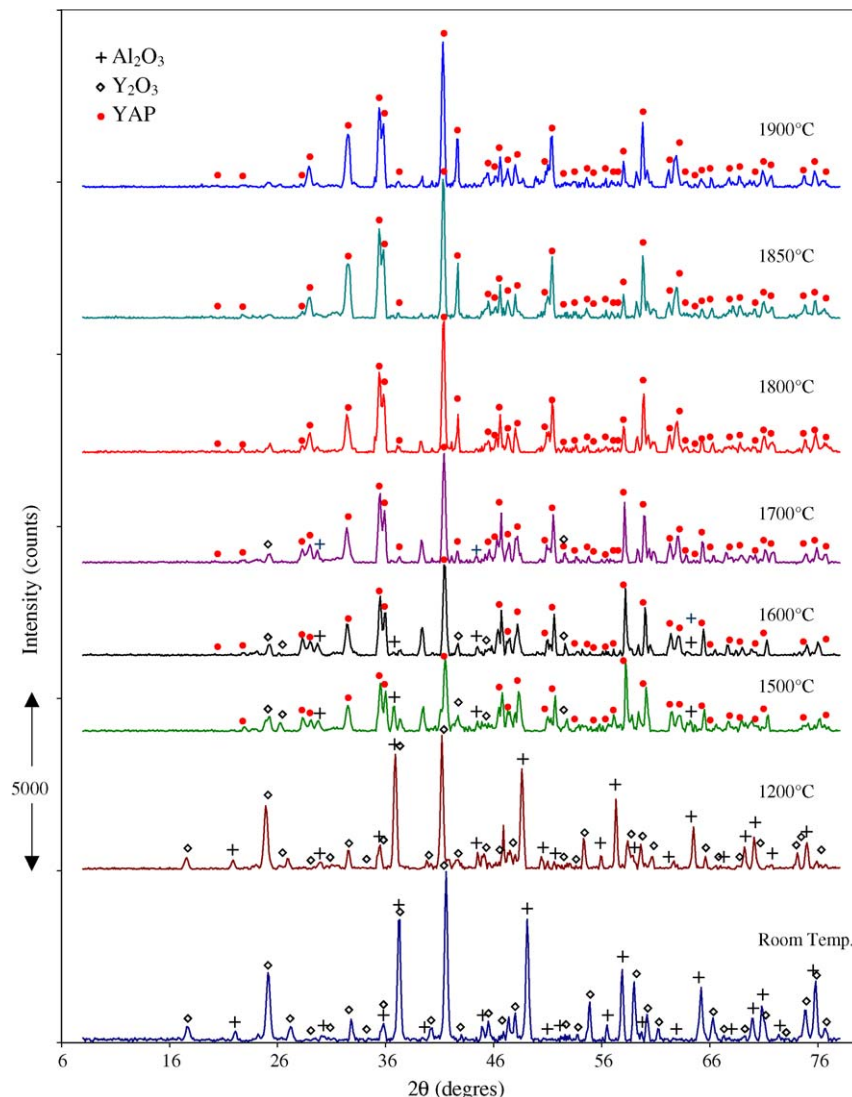


Fig. 8. Neutron diffractograms of heating of YAP composition.

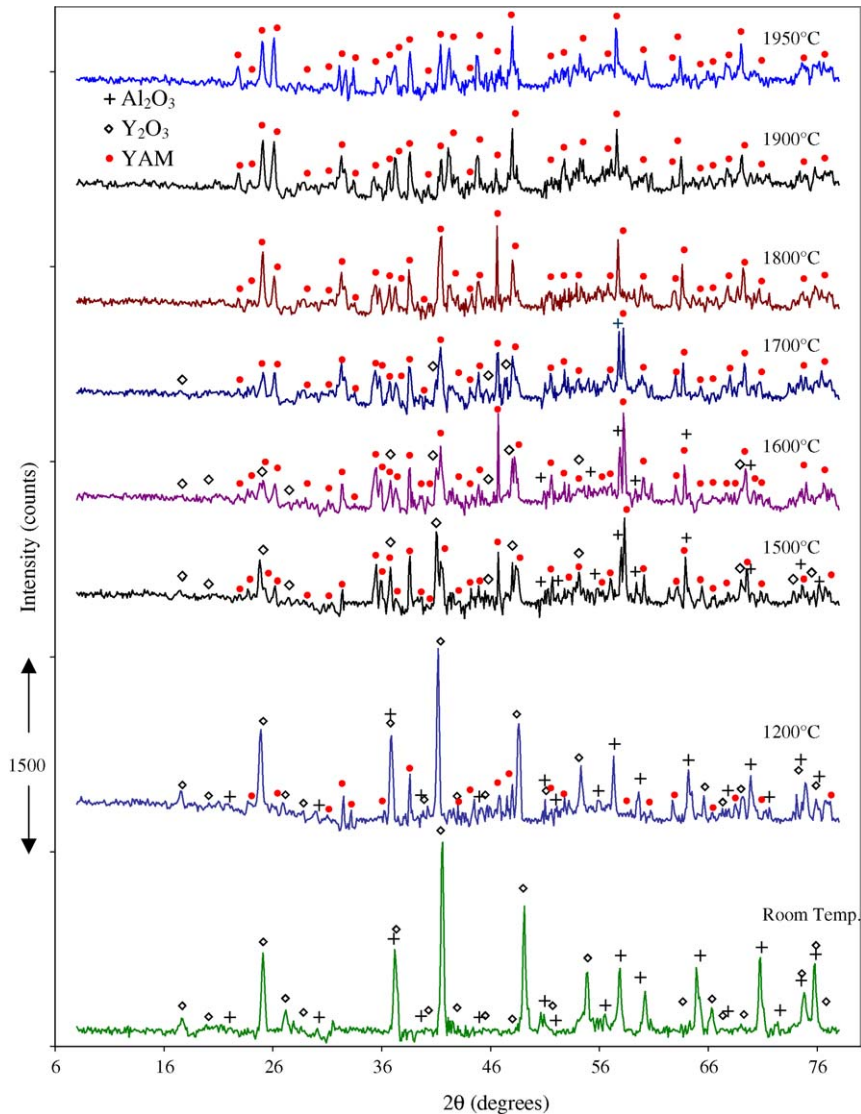


Fig. 9. Neutron diffractograms of heating of YAM composition.

starting material peaks and the growth of new peaks that were found to belong to YAP. Following the reaction in later stages of heating shows that this mixture provided a pure YAP phase by 1800 °C. This is because there are still  $\text{Al}_2\text{O}_3$  and  $\text{Y}_2\text{O}_3$  traces visible at 1600 °C and 1700 °C which however indicates that the reaction was complete in the temperature range 1700–1800 °C. Other evidence of incomplete reaction at 1700 °C is the growth of (2 3 0) peak of YAP at 42° ( $2\theta$ ). It can be seen that this peak did not get its full height below 1800 °C. Also, decaying of the (4 0 0) YAP peak at 59°, which overlaps with (7 2 3)  $\text{Y}_2\text{O}_3$  peak, proves indeed that some residual  $\text{Y}_2\text{O}_3$  exists at 1700 °C. From 1800 °C to 1900 °C the patterns were unchanged except for small shift in the peaks positions due to the thermal expansion of YAP unit cell.

During the course of in situ high temperature neutron diffraction experiments it was at times difficult to reach 2000 °C and to maintain the furnace at such high temperature. This resulted in starting the cooling cycle before melting took place. During the heating of this sample the furnace only reached 1900 °C. Even

though the melting point was not shown it can be said that the melting temperature of this sample is higher than 1900 °C.

During cooling from 1900 °C to room temperature, the patterns were practically unchanged. This clearly indicated that under these conditions the orthorhombic YAP phase is stable phase down to room temperature. Moreover, this was supported by reheating this compound for 3 h at 1550 °C to detect any high temperature decomposition. The resulting X-ray diffractograms of this compound before and after the heat treatment showed no difference and both belong to the orthorhombic crystal structure.

### 3.5. YAM composition

The development of the neutron diffraction pattern with increasing temperature up to 1950 °C of YAM composition (sample 5) is shown in Fig. 9. The first changes for this sample can be noticed by comparing the neutron diffraction patterns of 1200 °C and that of room temperature. There are additional peaks, which appear at 1200 °C. Although traces of YAM were

Table 2  
Summary of the results

Sample no.	Neutron diffraction results				Phase diagram <sup>25</sup>	
	Reaction started ( $T_{rs}$ )	Reaction finished ( $T_{rc}$ )	Melting temperature ( $T_m$ )	Stable phases	Melting temperature (°C)	Stable phases
1	$T_{rs} < 1200\text{ °C}$	$1200\text{ °C} < T_{rc} < 1500\text{ °C}$	$1850\text{ °C} < T_m < 1900\text{ °C}$	Al <sub>2</sub> O <sub>3</sub> and YAG	1820	Al <sub>2</sub> O <sub>3</sub> and YAG
2	$T_{rs} < 1200\text{ °C}$	$1500\text{ °C} < T_{rc} < 1600\text{ °C}$	$1950\text{ °C} < T_m < 2000\text{ °C}$	YAG	1942	YAG
3	$1200\text{ °C} < T_{rs} < 1500\text{ °C}$	$1500\text{ °C} < T_{rc} < 1600\text{ °C}$	$1950\text{ °C} < T_m < 2000\text{ °C}$	YAG and YAP	1908	YAG and YAP
4	$1200\text{ °C} < T_{rs} < 1500\text{ °C}$	$1700\text{ °C} < T_{rc} < 1800\text{ °C}$	$T_m > 1900\text{ °C}$	YAP	1915	YAP
5	$T_{rs} < 1200\text{ °C}$	$1700\text{ °C} < T_{rc} < 1800\text{ °C}$	$T_m > 1950\text{ °C}$	YAM	1978	YAM

seen at 1200 °C, formation of pure YAM from a mixture of 33 mol% Al<sub>2</sub>O<sub>3</sub> and 67 mol% Y<sub>2</sub>O<sub>3</sub> was not observed at a temperature lower than 1800 °C. This indicates that the reaction was completed in the temperature range of 1700–1800 °C. YAM peaks were identified according to the calculated pattern as monoclinic (space group  $P2_1/c$ ,  $a = 7.4706(5)\text{ Å}$ ,  $b = 10.535(6)\text{ Å}$ ,  $c = 11.1941(8)\text{ Å}$ ,  $\beta = 108.888^\circ(5)$ ).<sup>24</sup>

Patterns at 1800 °C, 1900 °C and 1950 °C are similar. Although the furnace reached 2000 °C for this sample, due to technical problems it was not possible to be maintained for a long time to collect the pattern of this temperature. Hence the cooling sequence started after staying 5 min at 2000 °C. It can be seen that the sample is still diffracting at 1950 °C. This leads to the conclusion that the melting temperature of sample 5 is higher than 1950 °C.

The neutron diffraction pattern of the cooling sequence for sample 5 shows that YAM is a stable phase from 1950 °C down to room temperature.

X-ray diffractograms indicate that reaction and formation of YAM takes place at 1500 °C for 2 h but this reaction is incomplete. This is consistent with the neutron diffraction results of this composition where the formation of YAM was not complete until 1800 °C. The starting powder reacted completely in the liquid state leading to the desired product being formed.

Table 2 summarizes the results of neutron diffraction experiments and compares them with the phase diagram of Al<sub>2</sub>O<sub>3</sub>–Y<sub>2</sub>O<sub>3</sub> system. It can be seen that the phases evolved at room temperature after heating and cooling of the different compositions are in complete agreement with the phase diagram. Whereas the melting temperatures measured in this work were generally higher than those indicated on the phase diagram shown in Fig. 1. Furthermore, YAP, YAG and YAM compounds have been observed as stable phases down to room temperature; this in turn should clarify any speculation regarding their decomposition. Also, this study showed that the formation of these compounds is possible through two different routes; melt extraction or solid-state reaction. In the latter case the temperature ranges for the reactions were provided.

#### 4. Conclusion

The present research was conducted to investigate the Al<sub>2</sub>O<sub>3</sub>–Y<sub>2</sub>O<sub>3</sub> binary system and from the results the following conclusions can be drawn:

1. High temperature neutron diffractometry has made it possible to follow, in real time, the reactions and especially the temperature range of each reaction involved in Al<sub>2</sub>O<sub>3</sub>–Y<sub>2</sub>O<sub>3</sub> phase diagram, which would have been impossible to determine ex situ.
2. Unique dynamic determination of the formation and melting temperatures of the stoichiometric compounds, YAG, YAP and YAM in Al<sub>2</sub>O<sub>3</sub>–Y<sub>2</sub>O<sub>3</sub> was established successfully in this study. The formation of these compounds started at around 1200 °C and finished by 1600 °C for YAG and by 1800 °C for both YAP and YAM.
3. The Al<sub>2</sub>O<sub>3</sub>–Y<sub>2</sub>O<sub>3</sub> binary phase diagram was investigated using X-ray diffraction for the different compositions. The results are in excellent agreement with the neutron diffraction results.

#### References

1. Medraj, M., Hammond, R., Thompson, W. T. and Drew, R. A. L., *J. Am. Ceram. Soc.*, 2003, **86**(4), 717–726.
2. Lo, J. and Tseng, T., *J. Mater. Chem. Phys.*, 1998, **56**(1), 56–62.
3. Gröbner, J., Lukas, H. L. and Aldinger, F., *Z. Metallkd.*, 1996, **87**(4), 268–273.
4. Abell, J. S., Harris, I. R., Cockayne, B. and Lent, B., *J. Mater. Sci.*, 1974, **9**(4), 527–537.
5. Cockayne, B., *J. Less-Common Met.*, 1985, **114**(1), 199–206.
6. Mah, T. and Petry, M. D., *J. Am. Ceram. Soc.*, 1992, **75**(7), 2006–2009.
7. Jin, Z. and Chen, Q., *CALPHAD*, 1995, **1**(19), 69–79.
8. Maier, A. and Savinova, I. G., *J. Inorg. Mater.*, 1996, **10**(32), 1078–1080.
9. Yamane, H., Omori, M. and Hirai, T., *J. Mater. Sci. Lett.*, 1995, **14**(8), 561–563.
10. Yamane, H., Omori, M., Okubo, A. and Hirai, T., *J. Am. Ceram. Soc.*, 1993, **76**(9), 2382–2384.
11. Yamane, H., Omori, M. and Hirai, T., *J. Mater. Sci. Lett.*, 1995, **7**(14), 470–473.
12. Gervais, M., Le Floch, S., Rifflet, J. C., Coutures, J. and Coutures, J. P., *J. Am. Ceram. Soc.*, 1992, **75**(11), 3166–3168.
13. Kerness, N. D., Hossain, T. Z. and McGuire, S. C., *Appl. Radial. Isot.*, 1997, **48**(1), 5–9.
14. Aguilar, E. A. and Drew, R. A. L., *J. Eur. Ceram. Soc.*, 2000, **20**(8), 1091–1098.
15. Sawada, H., *Mater. Res. Bull.*, 1994, **29**(2), 127–133.
16. Powder diffraction file, Card no. 10-0173, Joint Committee on Powder Diffraction Standards, Swarthmore, PA, 1998.
17. Sichinava, M. A., Kobayakov, V. P. and Taranovskaya, V. N., *J. Inorg. Mater.*, 1999, **9**(35), 965–968.

18. Gröbner, J., Kolitsch, U., Seifert, H. J., Fries, S. G., Lukas, H. L. and Aldinger, F., *Z. Metallkd.*, 1996, **87**(2), 88–91.
19. Faucher, M., *Acta Crystall. B*, 1980, **B36**(12), 3209–3211.
20. Hay, R. S., *J. Mater. Res.*, 1993, **3**(8), 578–604.
21. Hay, R. S., *J. Am. Ceram. Soc.*, 1994, **77**(6), 1473–1485.
22. Hay, R. S., *Mat. Res. Soc. Symp. Proc.*, 1995(357), 145–150.
23. Diehl, R. and Brandt, G., *Mater. Res. Bull.*, 1975, **10**(2), 85–90.
24. Nipko, J. C. and Loong, C. K., *Phys. Rev. B*, 1998, **57**(17), 10550–10554.
25. Roth, R. S., *Phase Equilibria Diagrams: Phase Diagrams for Ceramics, Vol XI*. The American Ceramic Society, Westville, OH, 1995, p. 107.